STAR Note 336

Analysis of Pulser Data from the 1997 TPC Cosmic-Ray Test

David Hardtke
Nuclear Science Division
Lawrence Berkeley National Laboratory
Berkeley, CA 94720

April 23, 1998

Abstract

Pulser data taken during the September, 1997 cosmic-ray test are analyzed. From these data, the relative gains are extracted. The various methods for extracting the gains are compared. The gain measurement rms is calculated, and found to be roughly 1%. The systematic variation of the relative gain is examined as a function of row, FEE board, and chip channel.

1 Data

For most sets of cosmic-ray test data, pedestal and pulser runs were performed before the cosmic data was taken. These runs were done primarily to extract online the pedestal for each pixel and relative gain for each pad. The pulser data can also be used offline to understand the systematics of the relative gains.

Two types of pulser data were taken. Most of the pulser data was taken by pulsing the ground wires. This induces an image charge on the pads. In addition, some runs were taken where charge was injected directly into the Front End Electronics. This note will examine only the ground wire pulser data. Two separate runs were examined. Tape 21, file 2 was for sector 19, while tape 25, file 8 was for sector 6. The electronics, however, were essentially the same for both runs.

The input signal and 9 outputs of the pad plane pulser are shown in figure 1. Each output drives a 50Ω load. A typical ADC reponse for the pad plane pulser is shown in Figure 2. This plot is for a pad in the outer pad rows. The reponses for the inner pads look very similar except that the maximum ADC is reduced. The upper plot shows all time buckets. The lower plot is the same histogram displayed in the region of the largest signal. The shaded area in the lower histogram shows the signal used the calculation of the "integrated" gain. The "peak" gain is simply the maximum ADC value. For this case, the integrated gain is 3542 and the peak gain is 549. By this definition, the gains are completely relative.

The online gain calculation is slightly different than the gain calculation used in this analysis. For the online gain calculation, all events in a given run are summed. Pedestal

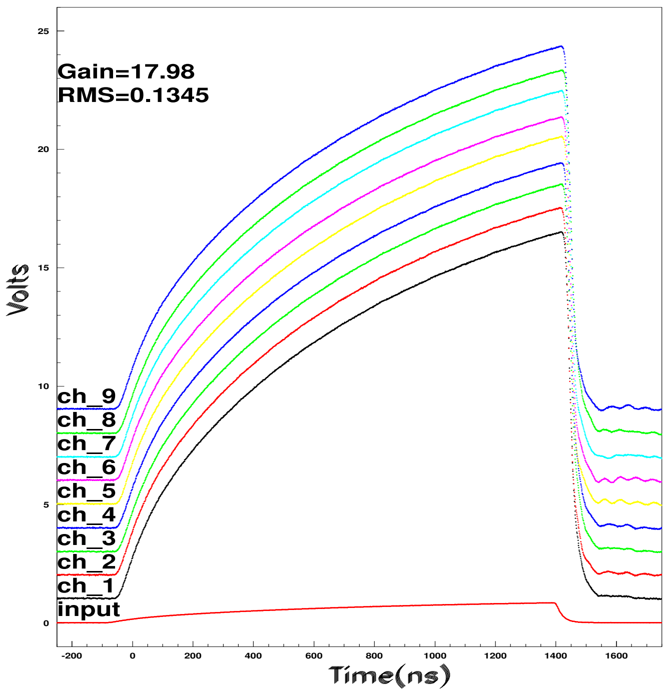

Figure 1: The input and 9 ouputs of the pad plane pulser. This figure is courtesy of Vahe Ghazikhanian.

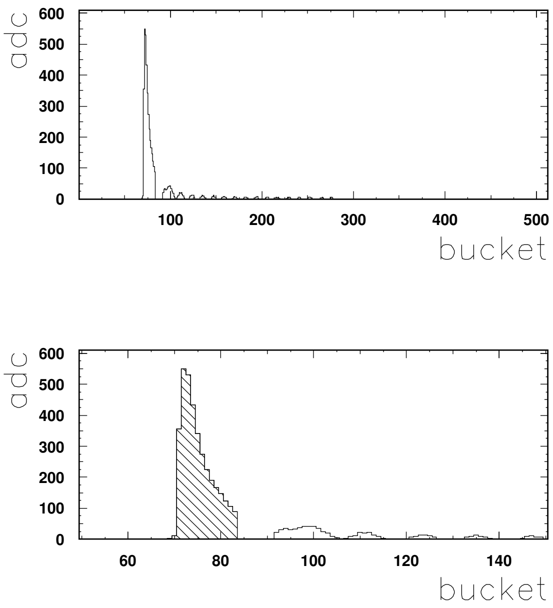

Figure 2: A typical ADC response from a pulser run for a typical pad in the outer sector. The upper plot shows all time buckets. The lower plot shows the time buckets near the pulse. The shaded area is the integrated gain.

subtraction is performed on the summed events. The peak of the summed ADC response is then found, and a search is done near the peak to find the positions where the signal falls below a threshold. The gain is then calculated by integrating over this region as well as a few buckets in the pre-sample and post-sample region. The number of buckets used online in the pre- and post-sample regions is an adjustable parameter, but it appears to have been set to 1. In the zero-supressed data used in the offline gain calculation, one pre-sample and one post-sample bucket is retained.

2 Peak vs. Integrated Gains

The calculated gain distributions as a function of row and pad are shown in Figure 3. The upper plot shows the average peak gain, while the lowel panel shows the average integrated gain. Note that for some pads the gain exceeds the values shown since the maximum ADC shown in these plots in 700 for the peak gain and 4500 for the integrated gain. The gains are generally well behaved except near the edges. For the outer (inner) pads, the rms deviation from the mean of the peak gain for all pads is approximately 4% (5%) of the mean. The rms of the integrated gains for the outer (inner) pads is 6% (8%) of the mean. Figure 3 also shows several interesting features that are easily understood. The effects of the outer sector edge pad geometry can be seen in the first pad of each row. Also, the chip structure (8 pads per chip) can be seen.

The mean peak gain is compared to the mean integrated gain in Figure 4. The two regions correspond to the inner pads (smaller ADC response) and outer pads. The relationship between the peak and integrated gain appears to be approximately linear for each sub-sector, but the linear relationship does not extrapolate to the origin. This effect is not understood.

3 Gain Measurement RMS

The online (relative) gain calculation is found by calculating the mean integrated pulser response. Since this takes time, it is desirable to know the RMS of the integrated pulser response and adjust the number of measurements accordingly. Figure 5 shows the integrated and peak pad response versus the event number for a typical pad in the outer sector. The rms of the single pad integrated response is approximately 1% of the mean in this case. The rms/mean is slightly worse for the peak response.

Figure 6 shows the single channel gain measurement rms/mean as a function of row and pad. Note the logarithmic scale on the z-axis. The upper plot shows the rms/mean for the peak response, and the lower plot shows the rms/mean for the integrated response. This single channel gain measurement RMS is approximately constant near the 1% level using both the peak response or the integrated response for both the inner and outer rows. There

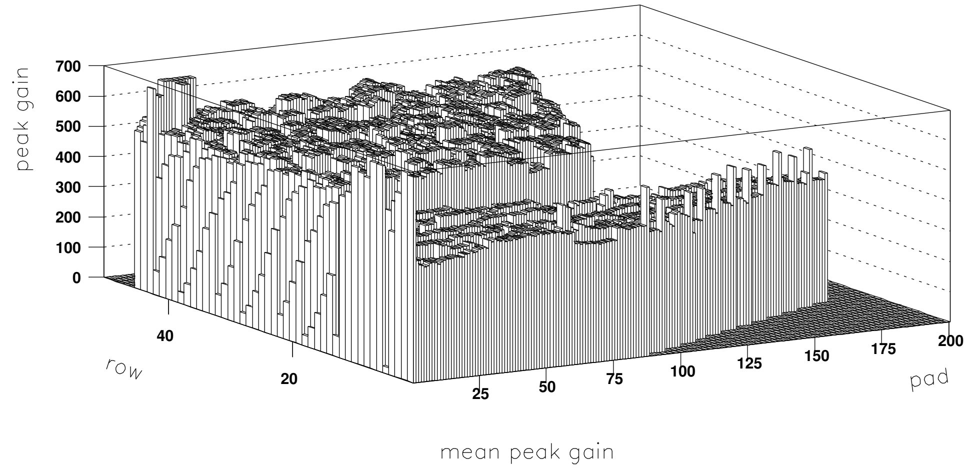

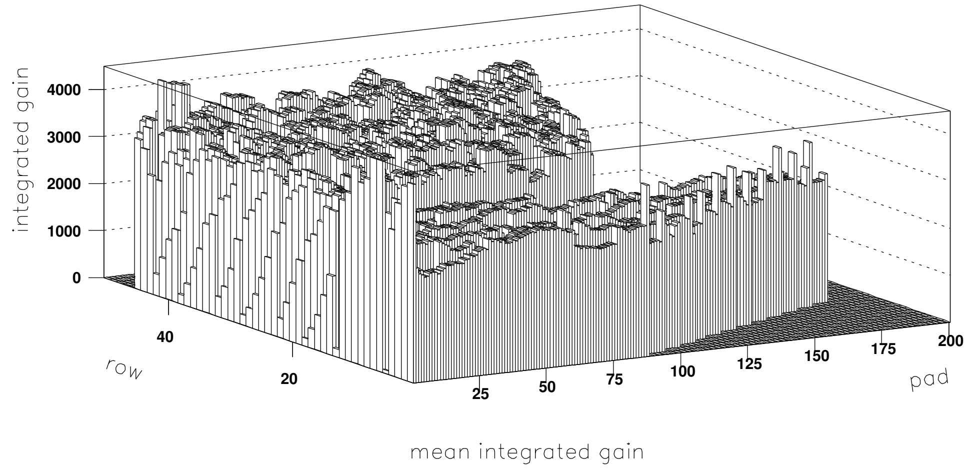

Figure 3: The calculated gain distributions from a pulser run (tape 21, file 2). The upper panel is the peak gain averaged over 53 events, and the lower panel is the integrated gain averaged over the same 53 events.

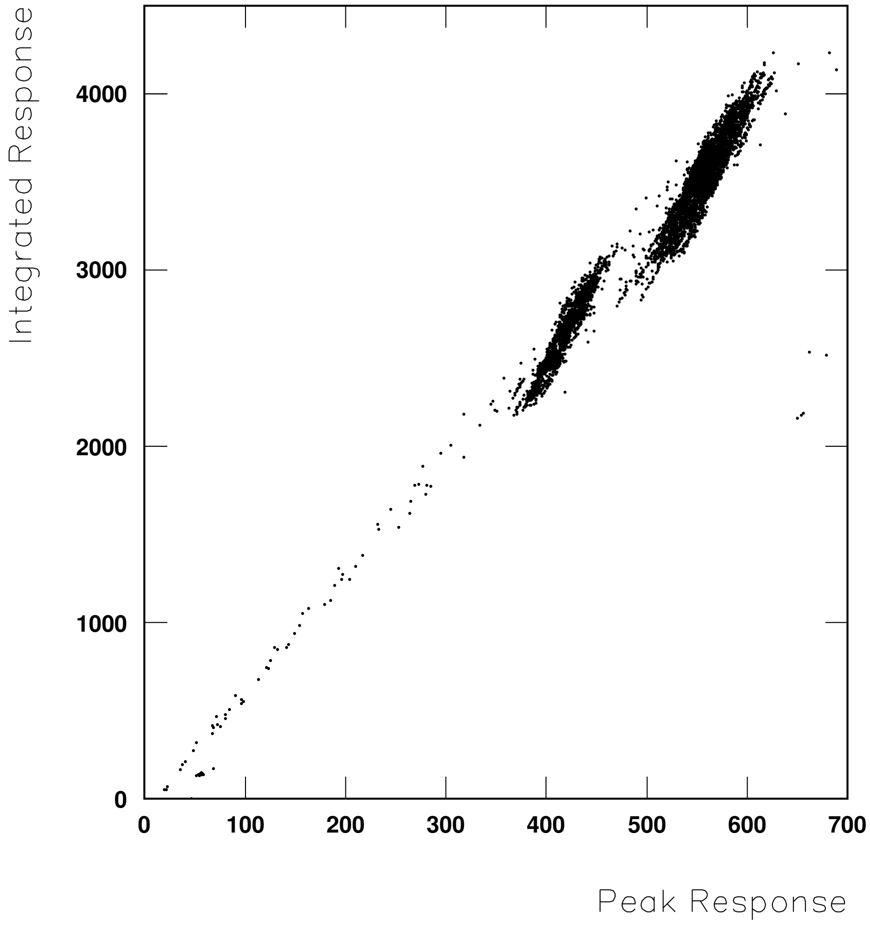

Figure 4: A scatter plot of the mean integrated gain versus the mean peak gain.

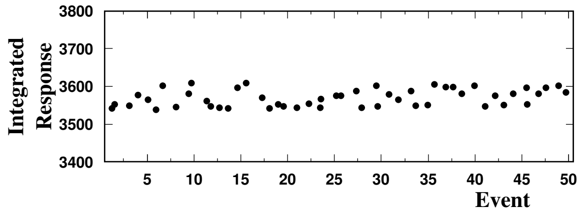

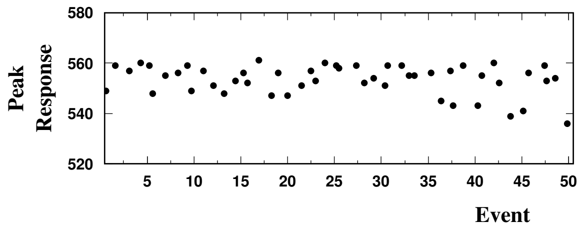

Figure 5: The integrated and peak pad response as a function of event number for a typical pad in the outer pad rows.

are a few pads, however, where the RMS/mean approaches 10%. There is a group of pads in row 4 (pads 73-88) that all have an rms/mean of 10%. The ADC response as a function of time bucket for one of these pads is shown in Figure 7. This should be compared to Figure 2. This particular cluster of bad pads are all on the same chip, suggesting a problem with this particular chip. This was later noted in the logbook (page 270), and this FEE board was replaced. A subsequent run showed no problems with these channels.

4 Chip Systematics

Figure 8 shows the distribution of integrated pad responses for chip 1 (upper plot) and chip 2 (lower plot). The distributions are only for the outer pad rows (rows 14-45). Also shown are the Gaussian fits to each distribution. The mean integrated pad response is roughly 40 ADC counts larger for chip 2. This represents a 1% systematic variation of the integrated pad response. A similar systematic 1% variation according to chip number exists for the inner pad rows (rows 1-13).

5 Row Systematics

In Figure 9, the average integrated gain for all pads in each row is plotted as a function of row. The error bars represent the RMS of the integrated gain distribution for that row. Edge pads are included in these calculations. This is plotted for two distinct pulser runs, and the two runs look very similar. For the inner rows, the fluctuations are large as a function of row, but there seems to be no particular trend. For the outer rows, however, there seems to be a slight dependence on row. It should be noted that a read-out board covers 8 rows (14-21,22-29, 30-37, 37-45). Hence some of the structure seen in the outer pad rows is probably due to the read-out boards (i.e. the higher gains in rows 14-21). Rows 22-45 seem to suggest that the gain increases slightly with row number, but this needs to be checked with another set of electronics.

6 Pad Response Near Sector Edges

The distortions of the electric field near the edges of the wire chambers lead to both a large variation in the gain and distortions of the position measurements. In Figure 3, it is clear that the edge pads in the outer rows show a reduction in the integrated pad response due to the geometry of the pads. In addition, there is a reduction in the pad response due to the electric field distortions. The inner rows show a different behavior. The edge pads show an increased pad response.

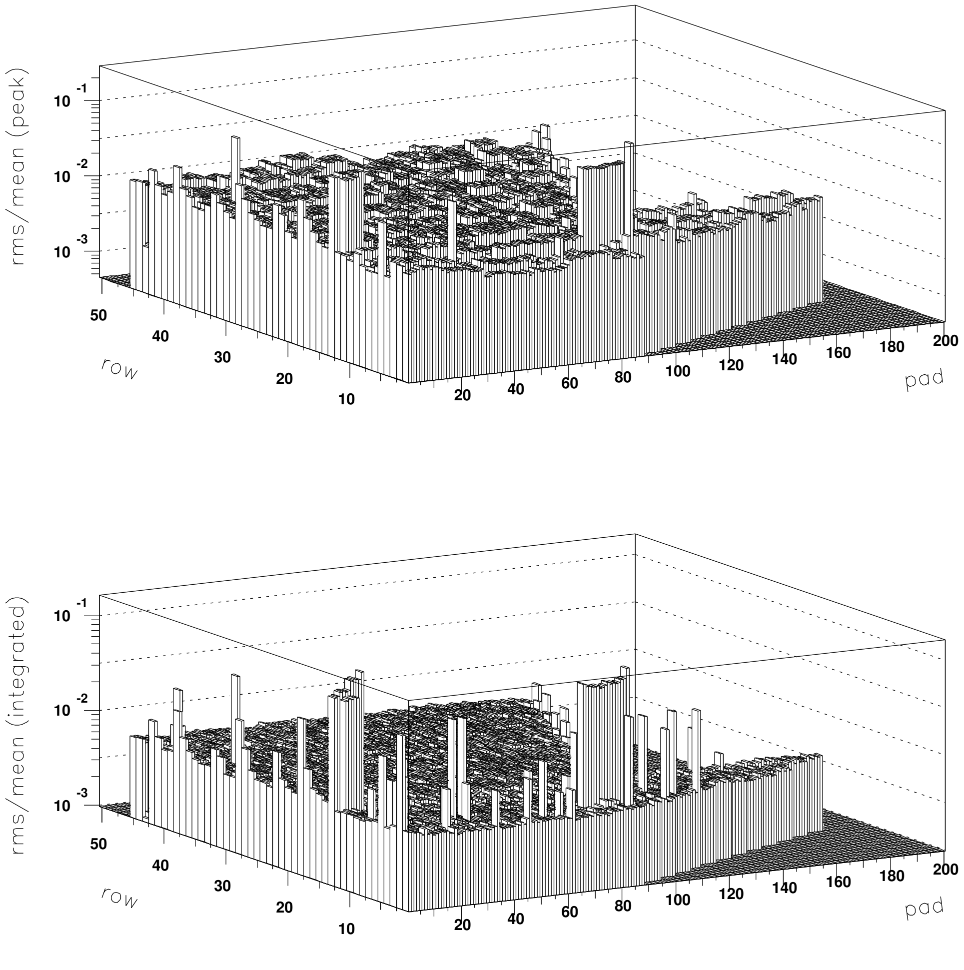

Figure 6: The RMS/mean of the peak (upper panel) and integrated (lower panel) pad response as a function of row and pad.

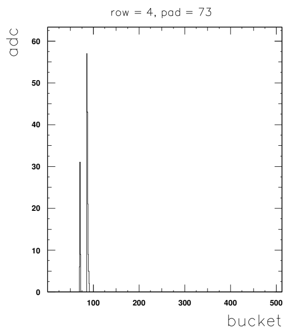

Figure 7: The ADC response as a function of time bucket for a bad pad.

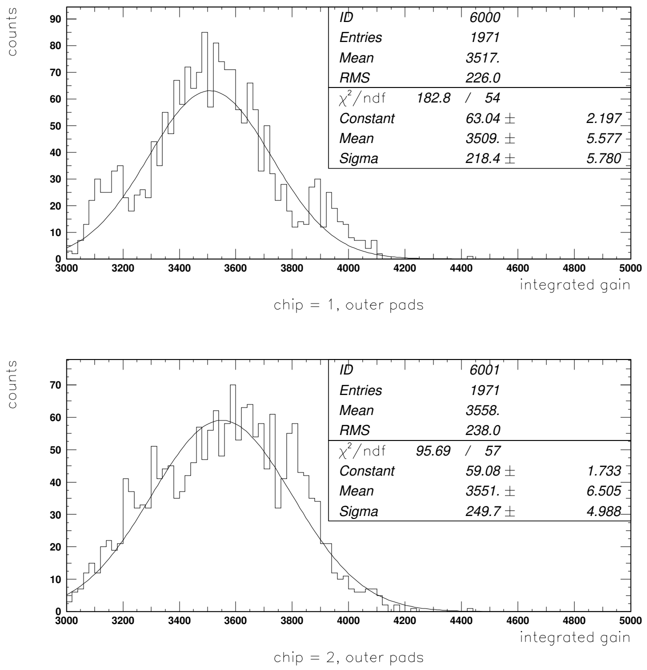

Figure 8: The distribution of the integrated pad response for chip 1 (upper plot) and chip 2 (lower plot). These plots are for the outer pad rows (rows 14-45).

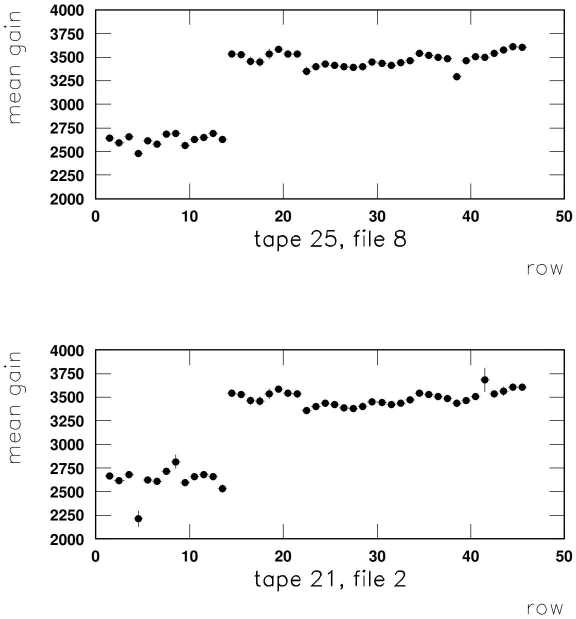

Figure 9: Profile histograms of the mean integrated gain as a function of row. The upper plot is from tape 25 and the lower panel is from tape 21.

Figures 10 and 11 show the integrated pad response for the 5 pads nearest the edge for a set of outer and inner rows, respectively. For the outer sub-sector (Figure 10), the first few pads and last few pads in each row show a reduced pad response. This is partially caused by the reduced pad area of pads at the end of the row. The open squares in Figure 10 show the "area corrected" integrated ADC response where the area corrected response is defined as

$$gain(area\ corrected) = gain(raw) \times \frac{nominal\ pad\ area}{pad\ area}. \tag{1}$$

The reduced pad area does not explain fully the reduced pad response near the sector edge.

For the inner subsector pad rows shown in Figure 11, the first pad has a larger integrated response than the other pads. For the other pads in the inner subsector, the systematics are not clear. Also plotted in Figure 11 are the relative pad areas normalized to 2000. The different behavior for the edge pads in the inner and outer subsectors may be related to the geometry of the wire chambers, but calculations of the electric fields near the edges of wire chambers may be needed to understand this behavior.

7 Conclusions

Pulser data from the cosmic-ray test data were analyzed. Various systematics of the relative gains were studied using the pulser data. The peak gain and integrated gain were compared, and found to follow similar trends. The overall gain RMS across all pads was found the be 5-8%, and RMS of the gain measurement on a single pad was found to be less than 1%. The gain was found to have a systematic 1% variation based on chip, and a stronger systematic variation based on read-out board. The edge pad response was found to differ for the inner and outer subsectors and not be explained by simple pad geometry.

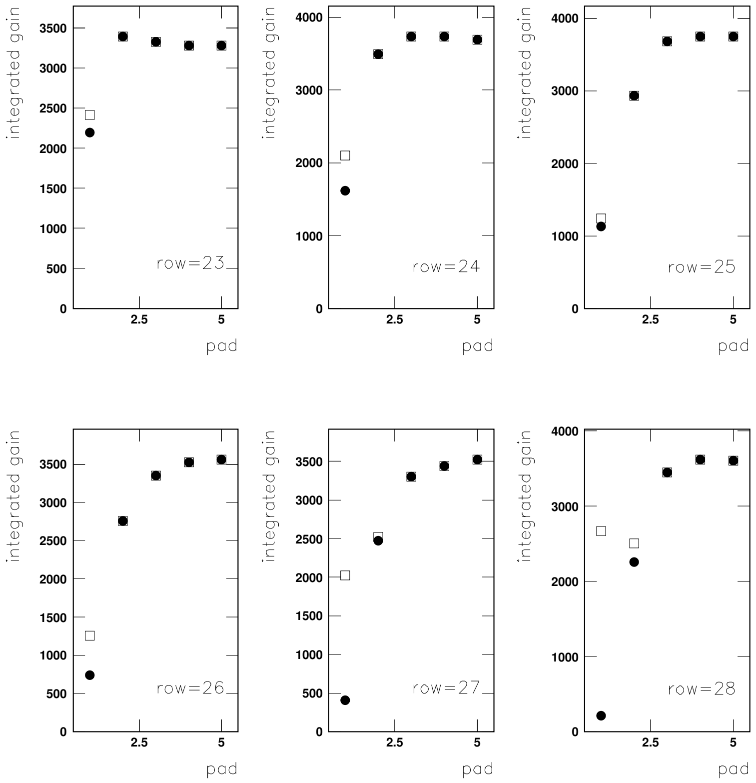

Figure 10: Integrated gain for pads 1-5 in rows 23-28 (solid circles). The open boxes show the integrated gain with a pad area correction.

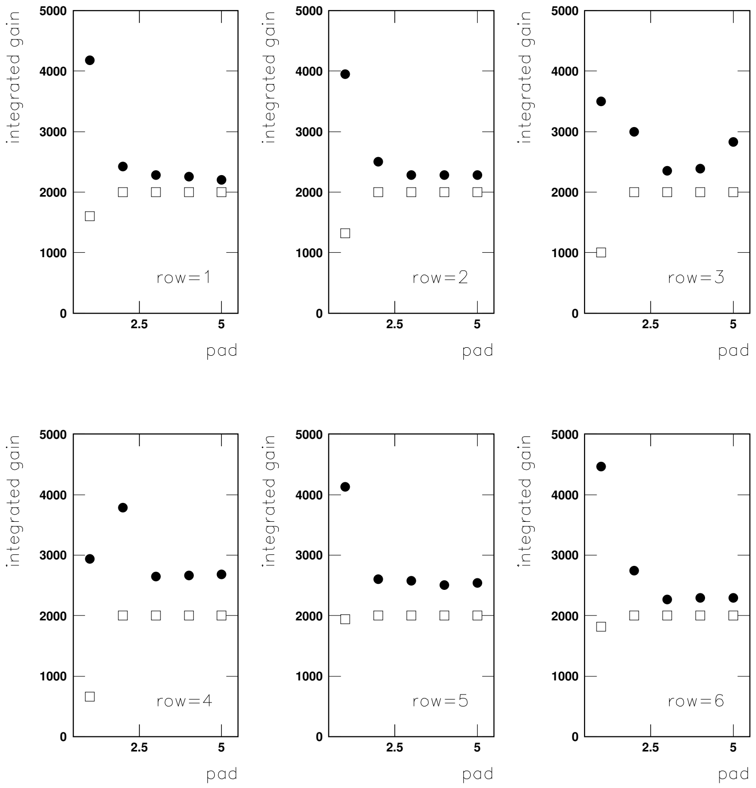

Figure 11: Integrated gain for pads 1-5 in rows 1-6 (solid circles). The open squares show the relative pad areas normalized to 2000.